Aircraft Ice Accretion Prediction Using Neural Network and Wavelet Packet Decomposition

S. Chang[a,*], M. Leng[a], H. Wu[b,**], M. Wu[a], J.M. Thompson[b]

[a]School of Aeronautic Science and Engineering, Beijing University of Aeronautics and Astronautics, Beijing 100191, China

[b]Institute of Engineering and Energy Technologies, School of Engineering, University of the West of Scotland, Paisley PA1 2BE, United Kingdom

[*]Corresponding author. Email: sn_chang@buaa.edu.cn Tel. (86)1082338008 Fax. (86)1082338008
[**]Corresponding author. Email: hongwei.wu@uws.ac.uk Tel. +44(0)1418483684 Fax.+44(0)1418483663

Abstract

A combined wavelet packet transform (WPT) and artificial neural networks (ANNs) modeling is developed for predicting the ice accretion on the surface of an airfoil. Wavelet packet decomposition is used to reduce the number of the input vectors to ANN and improves the training convergence. Artificial neural network is developed with five variables (velocity, temperature, liquid water content, median volumetric diameter and exposure time) taken as input data and one dependent variable (decomposed ice shape) as the output. For the purpose of comparison, three different artificial neural networks, back-propagation network (BP), radial basis function network (RBF), and generalized regression neural network (GRNN) are trained to simulate the wavelet packet coefficients as a function of the in-flight icing conditions. The predicted ice accretion shapes are compared with the corresponding results of NASA experiment, LEWICE and the Fourier-expansion-based method. Results show that the GRNN network has an advantage in predicting both the rime ice and glaze ice when the specimens are prepared using a separate method. Whereas the RBF network demonstrates a better performance in predicting the ice shape for the case of using the whole set of specimens. It is also found that WPT shows an advantage in performing the analysis of ice accretion information with high accuracy. The proposed model could be an efficient and a robust tool to predict aircraft ice accretion.

Keywords: Aircraft icing; Wavelet packet transform; Conformal mapping; Neural network

Nomenclature

c	chord length [inch]	ler	airfoil leading-edge radius [inch]
f	single-valued ice thickness functions [-]	LWC	liquid water content [$\mathrm{g/m^3}$]
$\bar{g}$	wavelet decomposition low-pass filter [-]	MVD	median volumetric diameter [μm]
g^*	wavelet reconstruction low-pass filter [-]	$Time$	time for the airfoil exposed to the icing condition [min]
$\bar{h}$	wavelet decomposition high-pass filter [-]	T_∞	free-stream static temperature [K]
h^*	wavelet reconstruction high-pass filter [-]	V_∞	free-stream velocity [$\mathrm{m/s}$]

1. Introduction

Aircraft icing has long been recognized for over sixty years and continues to be an important flight safety issue in the aerospace community. Ice accretion on an aircraft wing occurs when supercooled water droplets in the atmosphere impact on the surface of aircraft’s wings. The formation of ice on an aircraft wing results in a sharp increase in drag and a reduction in maximum lift. Furthermore, ice accretion on aircraft wings also leads to a reduction in stall angle and increment in moment coefficient of the wing. This causes a deterioration in the aerodynamic performance of the aircraft [1,2]. In terms of this, it is imperative to predict the ice accretion prior to designing reliable anti-icing/de-icing system. It is well recognized that several parameters, such as exposure time, liquid water content (LWC), median volumetric diameter (MVD), temperature, flight speed, angle of attack (AOA) and the chord length, play an dominate role in ice accretion. Droplets may freeze directly, building up rime ice or form a thin water film before freezing, and it may lead to glaze ice under certain conditions of high temperature and large LWC [3,4]. The former ice shape presents a smooth outline and can be simulated easily. Whereas the latter one usually exhibits uneven behaviour and may form two ice horns, which is more threatening to the flight safety [5].

Many efforts have been devoted to in-flight icing certification from both experimental and numerical aspects [6,7]. Icing wind tunnel testing usually provides most reliable data in fundamental study of aircraft ice accretion. Nevertheless, icing wind tunnel tests are very expensive and time consuming. It is thus not difficult to imagine that a CFD-based approach is desirable to save resources and to obtain relatively accurate results [8]. However, most of the models that are available rely on assumptions and simplifications that disagree at the real conditions of operation. In order to overcome these limitations, some researchers proposed a fast prediction method for aircraft icing through statistical strategy [9-11]. These efforts have achieved success in improving the icing prediction efficiency, but owning to the insufficiency and non-grid of the experimental data, a considerable computing time is still needed to obtain numerical simulation samples for the interpolation procedure.

The artificial neural networks (ANNs) technique offers an alternative approach for predicting the performance and generalizations of complex non-linear systems shortly. It is a method that is often used for predicting the response of a physical system that cannot be easily modeled. Neural networks have demonstrated the strong capability of learning non-linear and complex relationships between process variables without any prior knowledge of system behaviors. Ogretim et al. [12] achieved attractive performance with the neural network for predicting rime ice. ANN has been applied in modeling complicated relations or to find patterns in detection for in-flight icing characteristics [13], calibration of the multi-hole aerodynamic pressure probe [14], identification of the icing intensity [15], and predicting the effects of ice geometry on airfoil performance [16]. As data sets increase in size, their analysis become more complicated and time consuming. Thus, it is essential to reduce the size of data sets. The discrete wavelet transform (WT) is normally to analyze the irregular signals in view of its flexible time–frequency resolution [17]. However, WT can determine analysis only for low band frequency. As an extension of the WT, the wavelet packet transform (WPT) is capable of dividing the whole time-frequency plane while the classical [18-21]. For this reason, WPT will be considered in the current study.

The present study proposes a new methodology by the application of WPT and ANN to predict a 2D aircraft ice accretion. The paper is organized as follows: Section 2 recalls the conformal transform (CT), WPT and neural network techniques. Section 3 summarizes the results and observations. Finally Section 4 concludes the findings of this paper.

2. Algorithm and methodology

In this paper, the input data are converted to a single-valued signal using conformal transform (CT). Afterwards, the signal will be further analyzed through wavelet packet transform (WPT). Finally, the optimum artificial neural networks (ANNs) is selected as the target network. The schematic diagram of a combined WPT and ANN modeling is illustrated in Fig. 1.

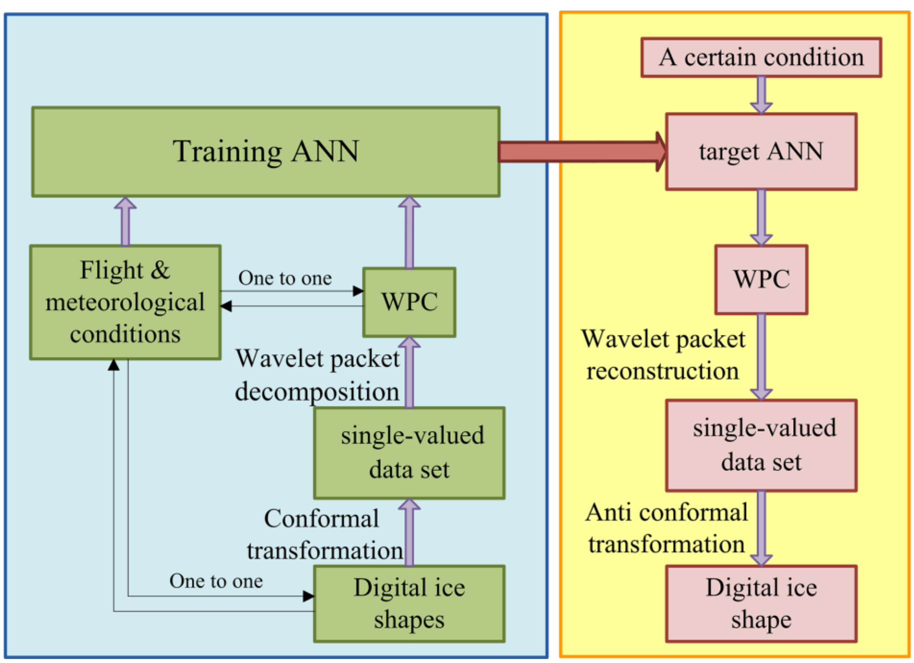

Fig. 1. The structure of intelligent modeling.

2.1. Conformal transform (CT)

Since the input data of the WPT must be single-valued, the coordinate of the original ice shapes are converted based on the conformal mapping method [22]. In the current study, the Cartesian coordinate system where the ice shape and airfoil originally exist is converted to the parabolic coordinate system where the ice shape will become a single-value function of abscissa. The leading-edge geometry of the airfoil with ice accretion is non-dimensionalized by the chord length, and then scaled by the non-dimensional airfoil leading-edge radius to coincide with the parabola:

$$x' = (x/c)/(ler/c) - 0.5, \quad y' = (y/c)/(ler/c) \tag{1}$$

where *ler* represents the airfoil leading-edge radius, and *c* is the chord length, $x - y$ is the original coordinate system and $x' - y'$ is the scaled coordinate system.

The parabolic shape and the ice accretion shape are illustrated in the same coordinate, as shown in Fig. 2. A conformal mapping is applied to transform the scaled physical $x' - y'$ plane to the $\xi' - \eta'$ plane by using Eq. (2):

$$x' = \frac{\xi'^2 - \eta'^2}{2}, \quad y' = \xi'\eta' \tag{2}$$

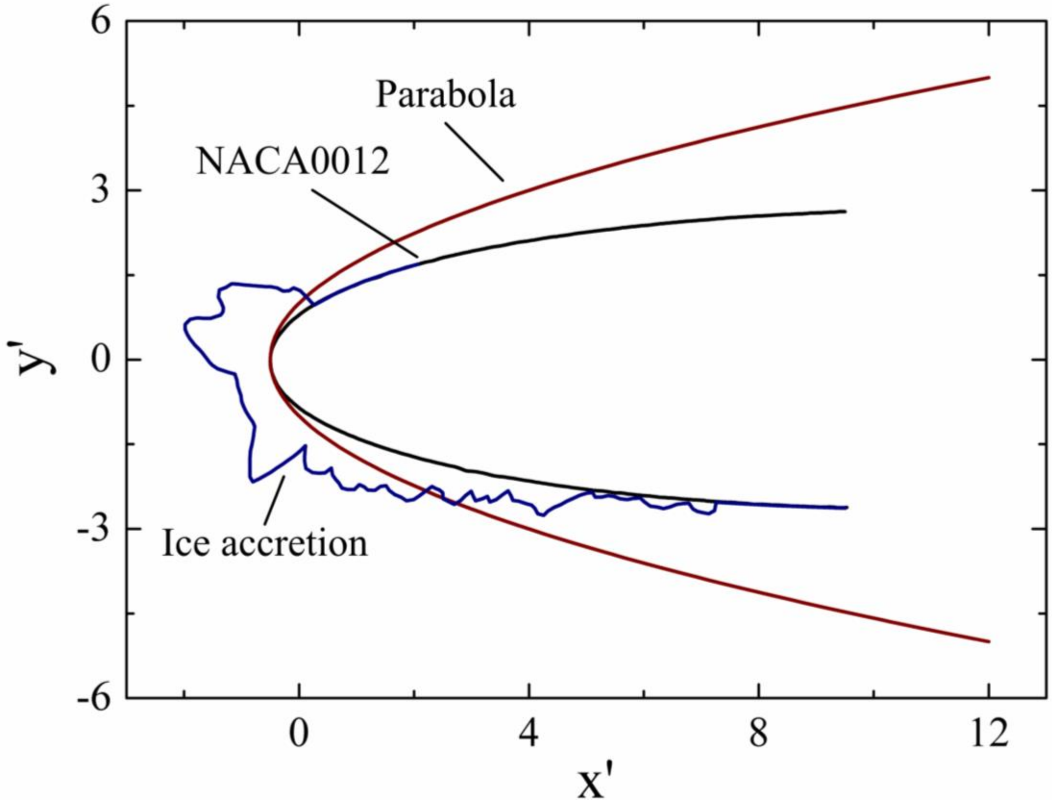

Fig. 2. Base parabola and scaled experimental ice shape in the x' - y' plane.

As a consequence, the parabola surface in the physical plane becomes a straight line and the airfoil with ice accretion can be seen as perturbations to the baseline parabola. The ice shape after conformal mapping is illustrated in Fig. 3. Following the conformal mapping, the Prandtl transposition is applied to separate the variables from the baseline:

$$\xi' = \xi, \;\; \eta' = \eta + f(\xi) \tag{3}$$

where $f(\xi)$ is an analytic expression representing all the perturbations at $\eta' = 1$. In order to normalize the specimens, the new coordinates of the ice shape in $\xi - \eta$ plane are obtained through linear interpolation. In this paper, the value of the abscissa is in the range from -4.38 to 2.0, and the space step is 0.02.

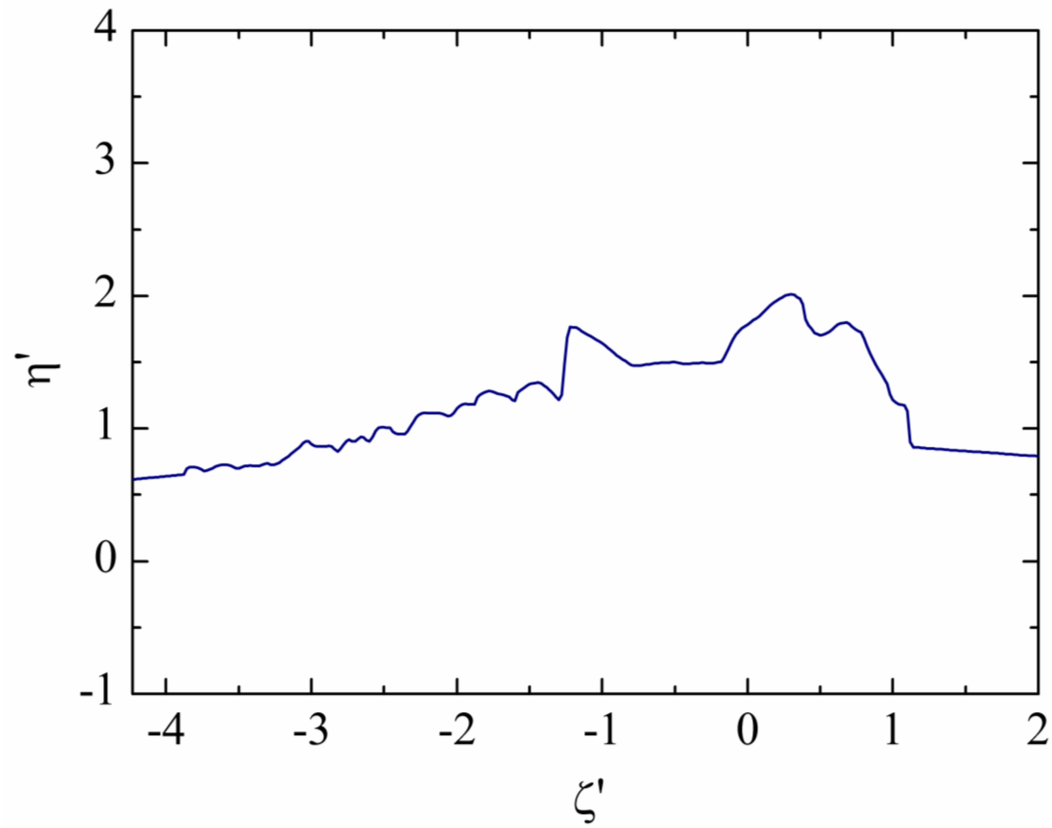

Fig. 3. Ice shape after conformal transform and its prolongation with airfoil.

2.2. Wavelet packet transformation (WPT)

Unlike the wavelet transform (WT), which is obtained by iterating the low pass branch, the wavelet packet transform (WPT) is obtained by iterating both low pass (approximation coefficients) and high pass branches (detail coefficients) at each level *j*. During wavelet packet decomposition procedure, both lower and higher frequency bands are decomposed into two sub-bands. Thereby wavelet packet gives a balanced binary tree structure. Fig. 4 shows a two level wavelet packet decomposition tree of an ice shape. For the *j*-level decomposition, the ice shape geometry after conformal transformation can be expressed as:

$$f(t) = \sum_{p=1}^{2^j} f_j^p(t) \tag{4}$$

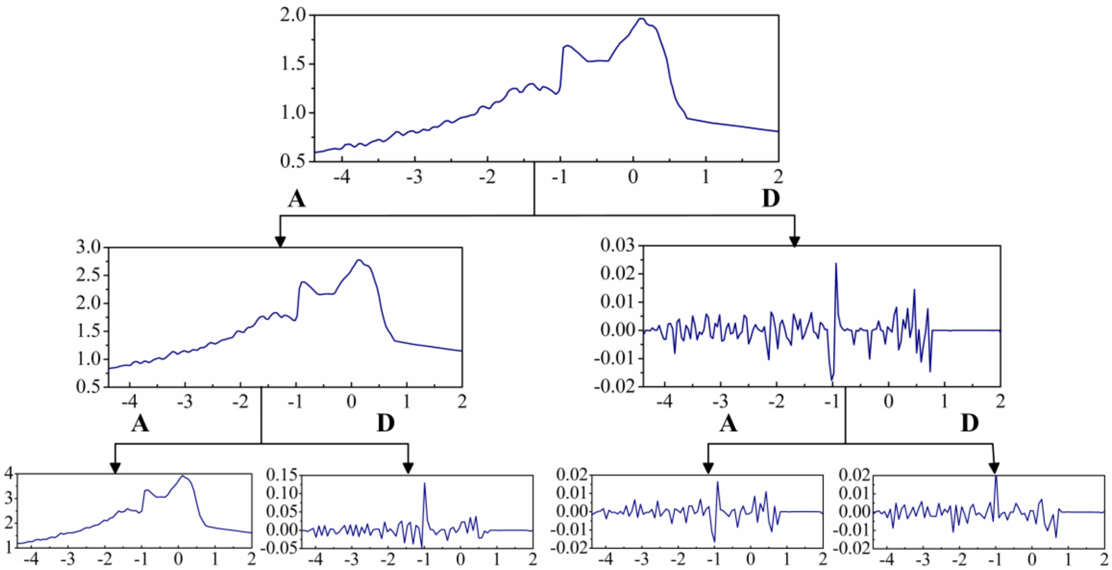

Fig. 4. Total decomposition tree of wavelet packet transform analysis.

Let $\bar{h}$ and $\bar{g}$ denote the high-pass filter and the low-pass filter, the remaining wavelet packet functions for p = 2, 3 …can be defined by the following recursive relationships:

$$\begin{cases} f_{j+1,k}^{2p-1}(t) = \sqrt{2} \cdot \sum_{k} \bar{h}(k-2t) \cdot f_{j,k}^{p}(t) \\ f_{j+1,k}^{2p}(t) = \sqrt{2} \cdot \sum_{k} \bar{g}(k-2t) \cdot f_{j,k}^{p}(t) \end{cases} \tag{5}$$

where the integers j and k are the index scale and translation operations, respectively. The index p is an operation modulation parameter or oscillation parameter. By iterating Eqs. (4) and (5) along the branches of the wavelet packet tree will compute the full wavelet packet decomposition. Then the wavelet packet component signal can be obtained with quadrature mirror filters. Different quadrature mirror filters can lead to different wavelet packet decompositions.

In the present study, both conformal mapping and WPT are applied to all experimental ice shapes to yield the corresponding wavelet packets coefficients. Since the order of the magnitude of the input data is large, normalization is implemented to make sure the input data within an appropriate range. After that, both the wavelet packet coefficients and the normalized icing conditions are used as the input to train the neural network. Once the target network is obtained, a group of data can be acquired as a function of the predicted icing condition, which will reconstruct an ice shape through the following reconstruction algorithm:

$$f_{j,k}^{p}(t)=\sum_{k} h^{*}(t-2k)\, f_{j+1,k}^{2p}(t)+\sum_{k} g^{*}(t-2k)\, f_{j+1,k}^{2p+1}(t) \tag{6}$$

where h^* and g^* are the reconstruction filters associated with the decomposition filters.

2.3. Artificial neural networks (ANN)

Artificial neural network (ANN) is a mathematical algorithm that highly interconnected the input and output parameters, learning from examples through iteration, without requiring a prior knowledge of the relationship of the process parameters. ANN is not new in concept, but research interest in this research area has increased significantly in the last two decades. The major reason for this interest is the short computing time and a high potential of robustness and adaptive performance. An artificial neural network is a computing system made up of simple interconnected processing elements called neurons. The neurons are interconnected by weighted links over which signals can pass and operate only on their local data and on the input they receive via the connections. The restrictions to local operations can often be relaxed during the learning process. ANNs should have specific training rules whereby the weights of connections are adjusted based on learning data. In other words, an ANN learns from examples (of known input/output sequences) and exhibits some capability for generalization beyond the training data. A network normally has great potential for parallelism, since the computations of the components are largely independent of each other. The function of each element is determined by its structure, connection strengths, and the processing performed at computing elements or nodes. The trained network is utilized in output prediction corresponding to a set of new inputs.

A sufficiently trained network is expected to produce outputs that are satisfactorily close to actual outputs.

In the current study, the available published experimental ice shapes from NASA icing wind tunnel will be used to train the neural network. During the training process, the network learns the wavelet packet coefficients of an ice shape as a function of the corresponding atmospheric and flight conditions. Fig. 5 shows an illustration of a typical multilayer feed-forward neural network. A total of five normalized icing condition variables (velocity, temperature, LWC, MVD and exposure time) are used as the input and decomposed ice shape as the output. If the wavelet packet decomposition process is taken for *j* times, there would be 2^j independent arrays, the length of which will be the 2^jth of the original length. In order to increase the training efficiency of the network, these 2^j groups of the wavelet packet coefficients are separated into 2^j different training sets. Once all the trainings are converged, the target network can be used to predict the ice shape through Eq. (6). For the purpose of balancing the efficiency and the accuracy, a parametric study to determine an optimum number of *j* is implemented. Four-level wavelet packet decomposition is recommended for the current study.

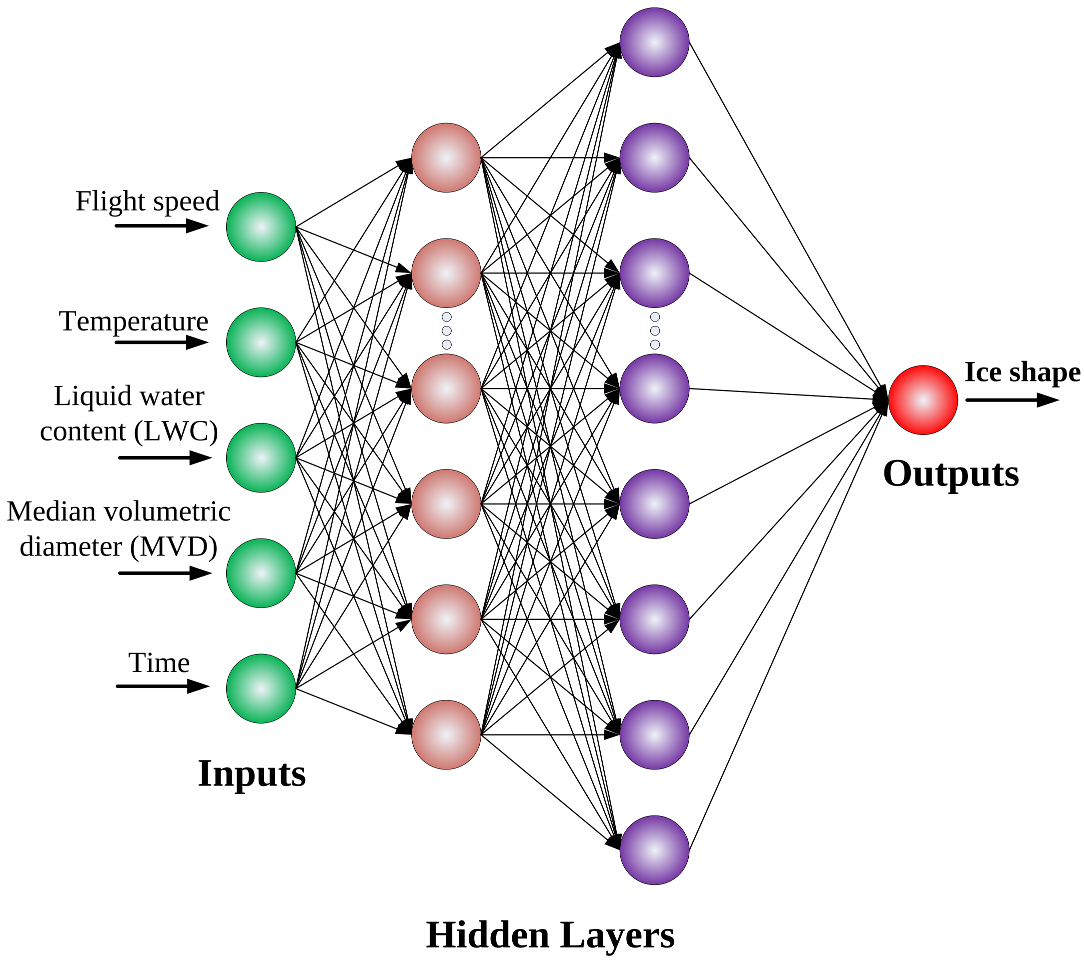

Fig. 5.

Schematic diagram of the artificial neural network structure.

In the current study, three different structures of ANN are selected to implement the prediction. They are back-propagation (BP) network, radial basis function (RBF) network and generalized regression neural network (GRNN). A comparative study is carried out in order to select an adequate neural network. The ANN is trained with the data from the experiments of the NASA Icing Research Tunnel (IRT) at NASA Glenn and the LEWICE validation report [23]. Four typical icing conditions that selected from the work of Ogretim et al. are listed in Table 1.

Table 1

Ice accretion input test data for ANN application.

Ice type	IRT run number	Velocity (m/s)	Static Temperature(K)	LWC (g/m3)	MVD (microns)	Icing Time (min)
Rime1	July 1996 20735	102.8	256.49	0.34	20	11.5
Rime2	July 1991 27-6-36	58.1	256.19	1.30	20	8
Glaze1	July 1996 21236	102.8	262.04	0.44	30	8.75
Glaze2	July 1996 21336	102.8	262.04	0.48	40	8

2.4. Error analysis

To evaluate the accuracy of the proposed algorithm, the quantitative comparison between the predicted ice shapes and the experimental results are conducted. The predicted results are also compared with that of LEWICE and the work of Ogretm et al. The relative cross-section area error is selected as the main criteria. The data points in the $\xi-\eta$ plane are utilized to represent the ice thickness since the perturbation $f(\xi)$ is a single-value function. The relative cross-section area error can be calculated by:

$$\%error=\frac{\sum_{i=1}^{N}\left|f_{e_i}-f_{p_i}\right|\Delta\xi_i}{\sum_{i=1}^{N}\left|f_{e_i}\right|\Delta\xi_i}\times 100\%=\frac{total\ area\ of\ error\ region}{total\ experimental\ ice\ area}\times 100\% \tag{7}$$

where the subscript e denotes the experimental ice thickness and the subscript p denotes the predicted ice thickness, N is the total number of data points, $\left|f_{e_i}-f_{p_i}\right|\Delta\xi_i$ is the area of the i-th rectangular element between the experimental and the predicted ice shape, $\left|f_{e_i}\right|\Delta\xi_i$ is the absolute cross-section area of the i*-th* rectangular element for the experimental ice shape. The selected method of the error calculation can successfully reflect the general performance of the prediction methods.

3. Results and discussion

3.1. Software interface for ice shape prediction

MATLAB Neural Network and Wavelet Toolboxes are used to build the network as well as an in-house ice prediction program is developed. Fig. 6 shows the screen shot of the developed software for predicting the ice shape based on WPT and ANN. Fig. 6 mainly consists four parts: flight conditions on the upper right, WPT and ANN option in the middle, data setting on the left, and results display window on the lower right. In the current study, five flight conditions, i.e. V_∞, T_∞, *LWC*, *MVD* and *Time*, need to be given before running the software. Then selecting the type of the database (“IceShape”) and the number of the wavelet packet decomposition layers (“WPDecLayer”), followed by activating the ice accretion prediction button. When clicking the “PredictExam”, the number of samples need to be selected as the target output. After running the simulation, the predicted ice shape will be plotted together with the experimental results and LEWICE for comparison, as illustrated in Fig. 6.

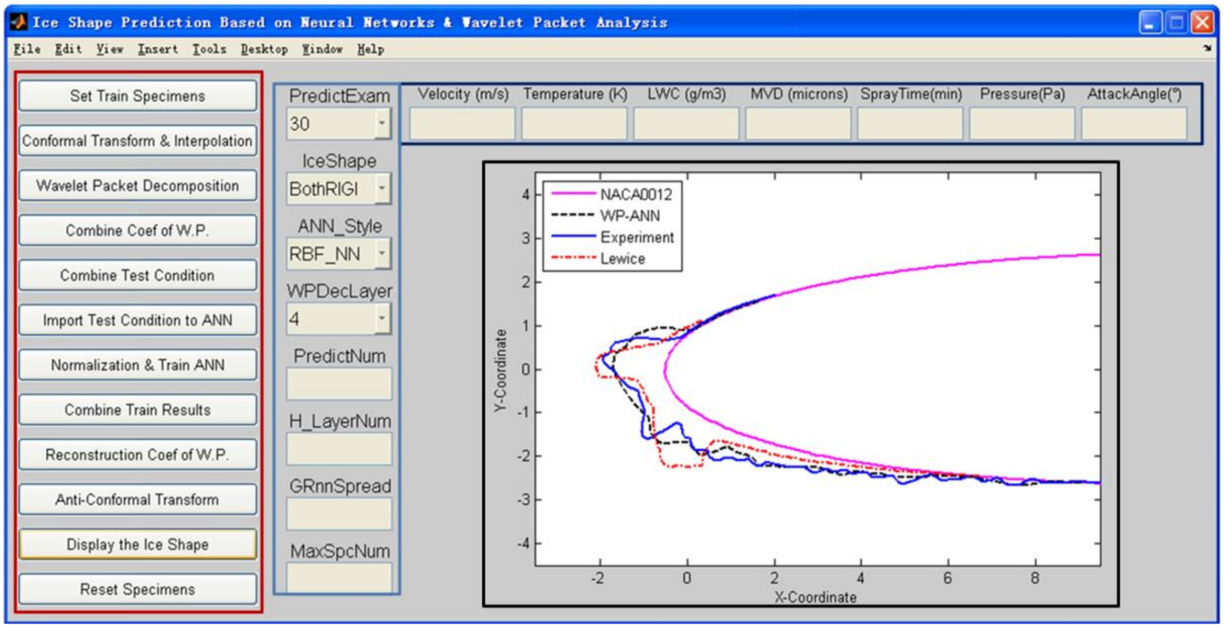

Fig. 6. The interface developed for the prediction of the ice shape.

To comprehensively evaluate the performance of the proposed methodology, the simulation will be conducted using both the separated-specimen method and the whole-set method [12]. The separated-specimen method is used to divide the ice shape database into the rime ice and the glaze ice, and the prediction will be carried out for each set. It is generally considered that the ice shape can be predicted using separated-specimen method with higher accuracy and efficiency. While the whole-set method will incorporate the whole set of specimens into the developed software and determine whether it is rime ice or glaze ice by the predicted results, which is thought more practical. For the purpose of comparison, in the current work, both the separated-specimen method and whole-set method will be tested.

3.2. Analysis with separated specimens

It is recognized that either rime ice or glaze ice has its unique characteristics. As is always the case, horns and excessive ice roughness normally show the behavior of glaze ice, whereas smooth geometry denotes rime ice. Since the current work only focuses on predicting the outer ice shape profile, the classification is taken in terms of the outer ice shape which is is similar to the work of Ogretim et al [12].

Figs. 7-10 show the comparison of the ice shapes (rime and glaze) of the experimental, LEWICE and present BP, RBF and GRNN result. It can be seen clearly from both Figs. 7 and 8 that the ice extension and ice shape of the leading edge is predicted better by both the BP and GRNN than that predicted by LEWICE. Although the maximum thickness of GRNN result for the second rime case is under-predicted, the location of the maximum thickness is fairly well predicted. A quantitative comparison of the neural network and LEWICE prediction results to the experimental results in terms of the relative cross-section area error is given in Table 2. Herein N.N. stands for the work of Ogretim et al. (combination of the Fourier expansion and ANN). From Table 2, it is observed that small fluctuation appeared in the BP network results. This may be attributed to the over-fitting, which could lead to a serious distortion when the whole set of the specimens are applied in training BP neural network. In contrast, both the RBF and GRNN network predicted ice shapes with smooth geometry.

Table 2

Summary of errors when using the separated specimens.

Ice type	Data file number	LEWICE Area error(%)	N.N. Area error(%)	BP Area error(%)	RBF Area error(%)	GRNN Area error(%)
Rime ice1	JULY 1996 20736	35.40	12.43	18.10	24.00	18.51
Rime ice2	JULY 1991 27-6-36	27.70	22.95	21.42	27.03	24.31
Glaze ice1	JULY 1996 21236	28.43	32.32	33.20	24.17	24.57
Glaze ice2	JULY 1996 21336	28.23	32.43	34.58	29.06	29.76

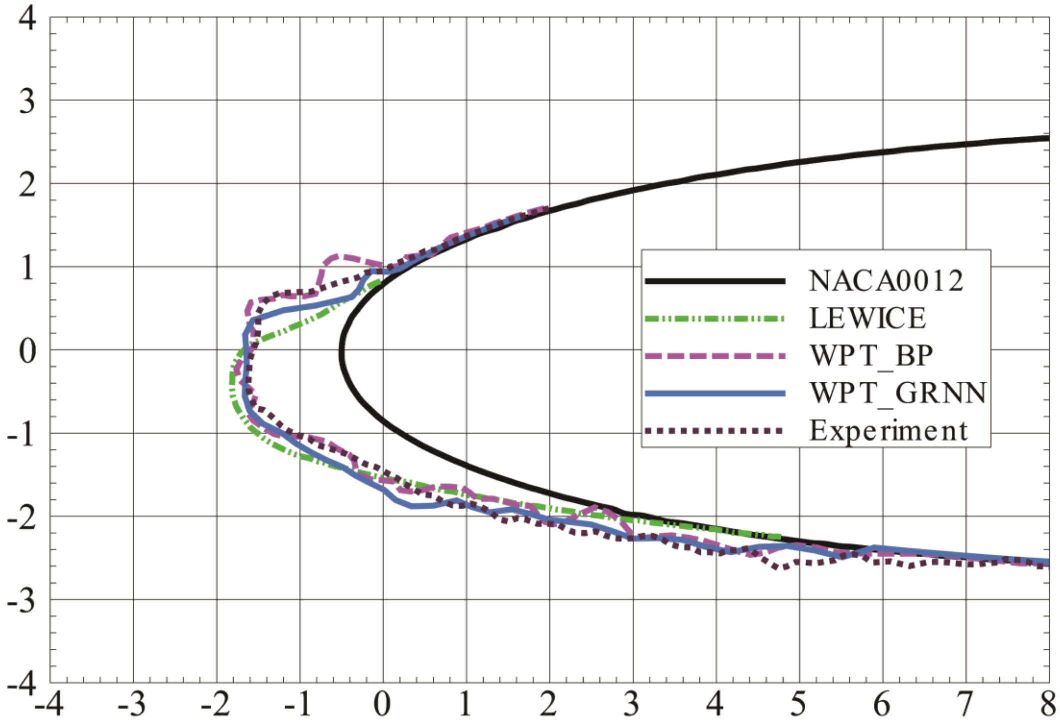

Fig. 7. Comparison of the rime ice1 shapes of the experimental, LEWICE and present BP and GRNN result.

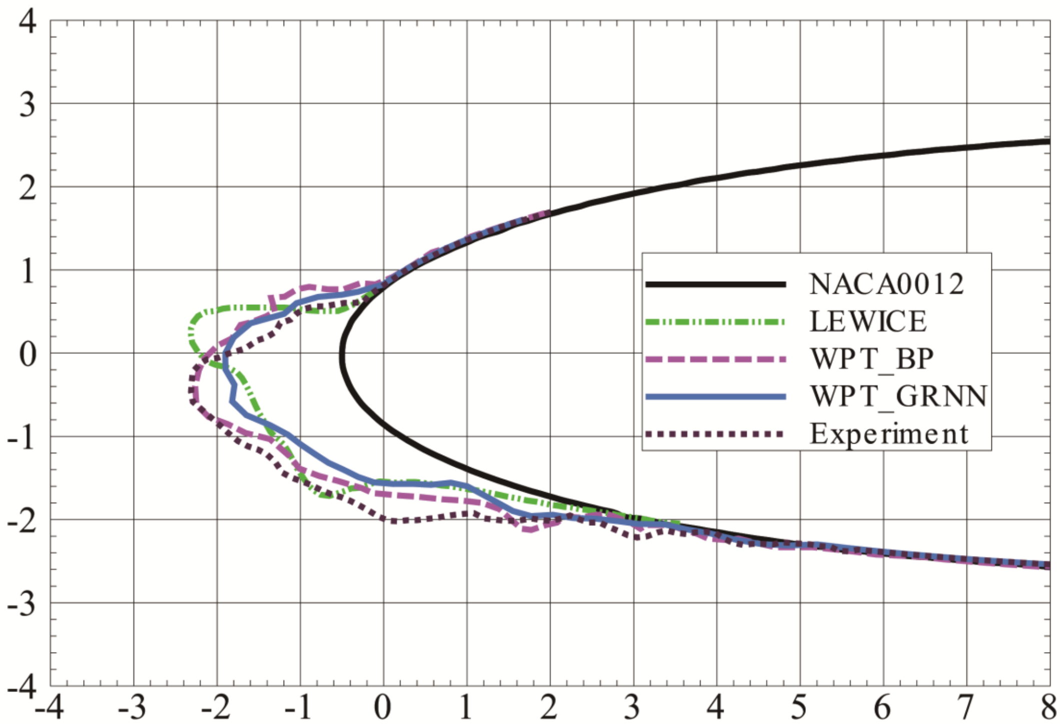

Fig. 8. Comparison of the rime ice2 shapes of the experimental, LEWICE and present BP and GRNN result.

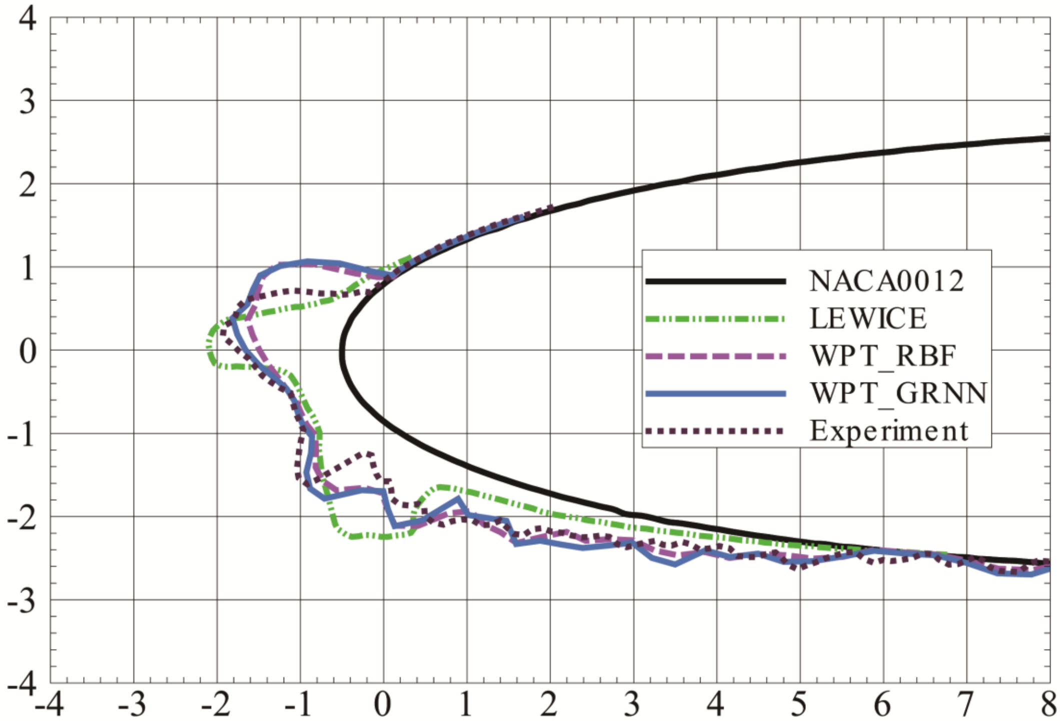

Fig. 9. Comparison of the glaze ice1 shapes of the experimental, LEWICE and present RBF and GRNN result.

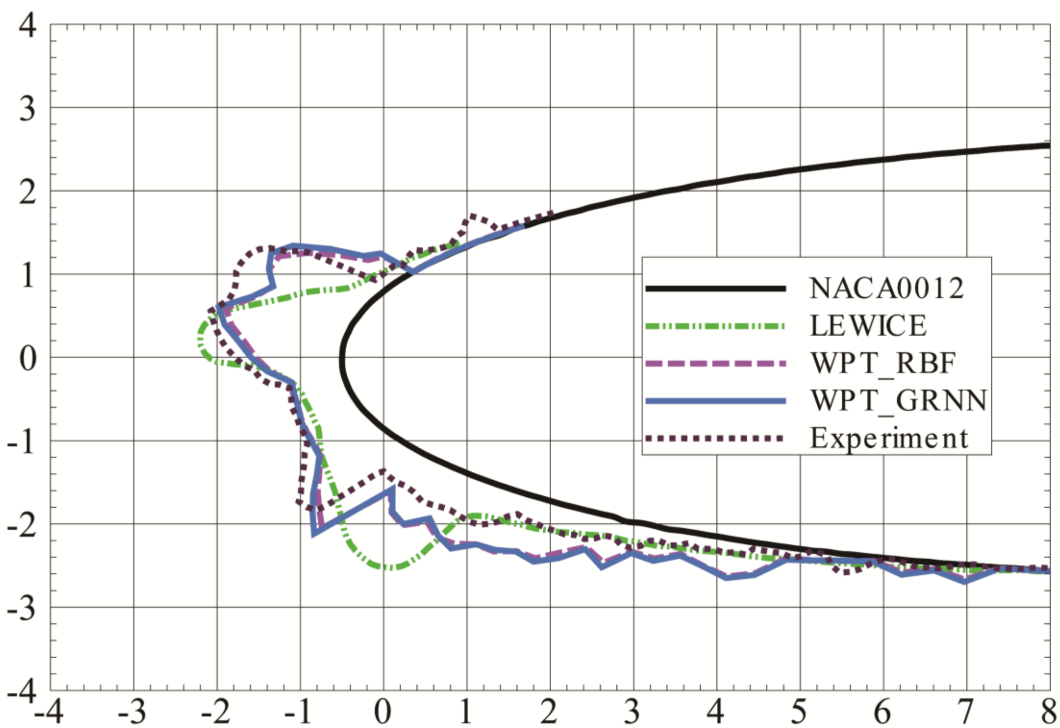

Fig. 10. Comparison of the glaze ice2 shapes of the experimental, LEWICE and present RBF and GRNN result.

Figs. 9 and 10 show a similar comparison for the case of glaze ice conditions. It is clearly observed that both the RBF and GRNN are able to satisfactorily predict the ice shape in terms of the location and height of the ice horns as well as the surface roughness. The extent of the ice shape on the lower side is also fairly well predicted. For the glaze ice cases, the ice mass predicted by GRNN and RBF are similar and both over predicted the experimental result. As an overall evaluation, the GRNN network demonstrates a better performance in predicting the ice shape for both the rime ice and glaze ice is clearly classified.

3.3. Analysis with the whole set of specimens

In this section, the whole set of the ice shape samples are implemented into the neural network as the input data. It is always not possible to know the type of the prediction ice conditions before ice accretion simulation since there is a considerable conditions in nature that cannot be simply determined. As a matter of fact, given the whole set of the specimens, the GRNN can keep the same accuracy compared to the predicted results using the separated-specimen method, whereas the RBF network even achieves better performance, as shown in Figs. 11-14. In general, the predicted ice horns are accurately captured and the surfaces of the predicted glaze ices are obviously rougher than that of the rime ices.

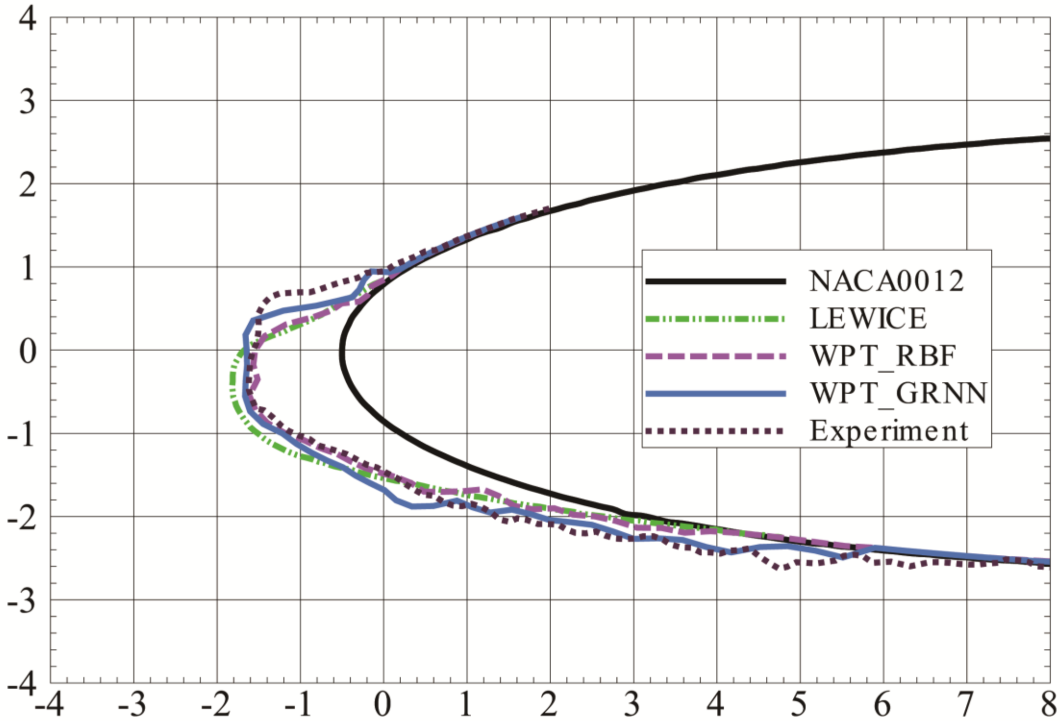

Fig. 11. Comparison of the rime ice1 shapes of the experimental, LEWICE and present RBF and GRNN result.

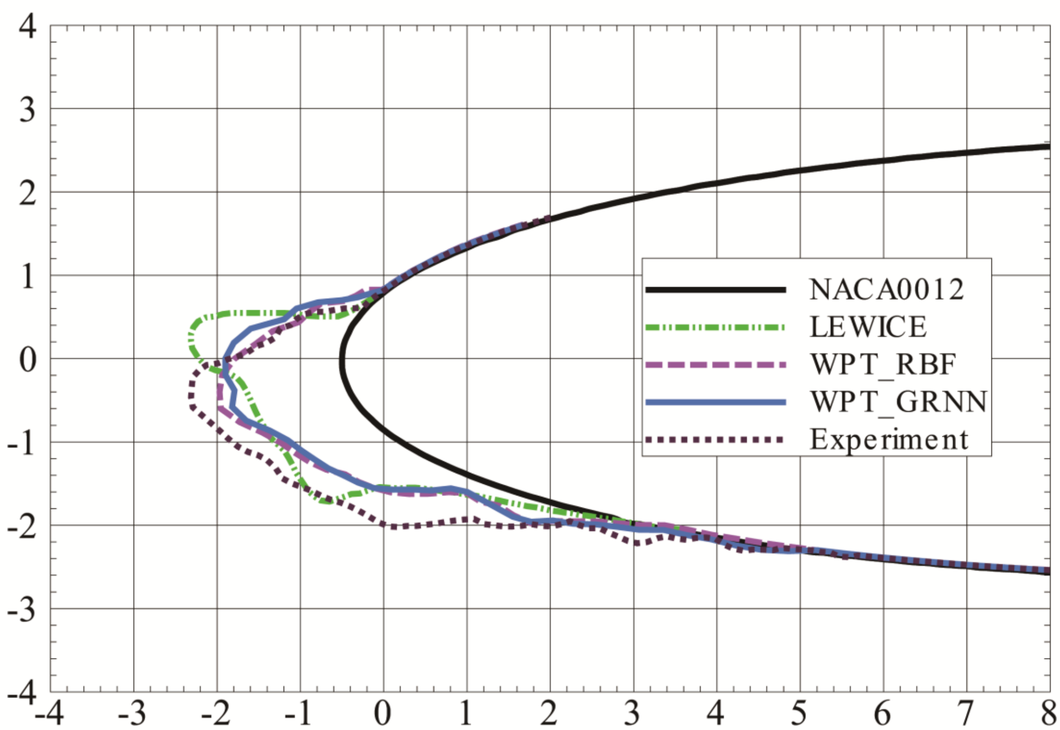

Fig. 12. Comparison of the rime ice2 shapes of the experimental, LEWICE and present RBF and GRNN result.

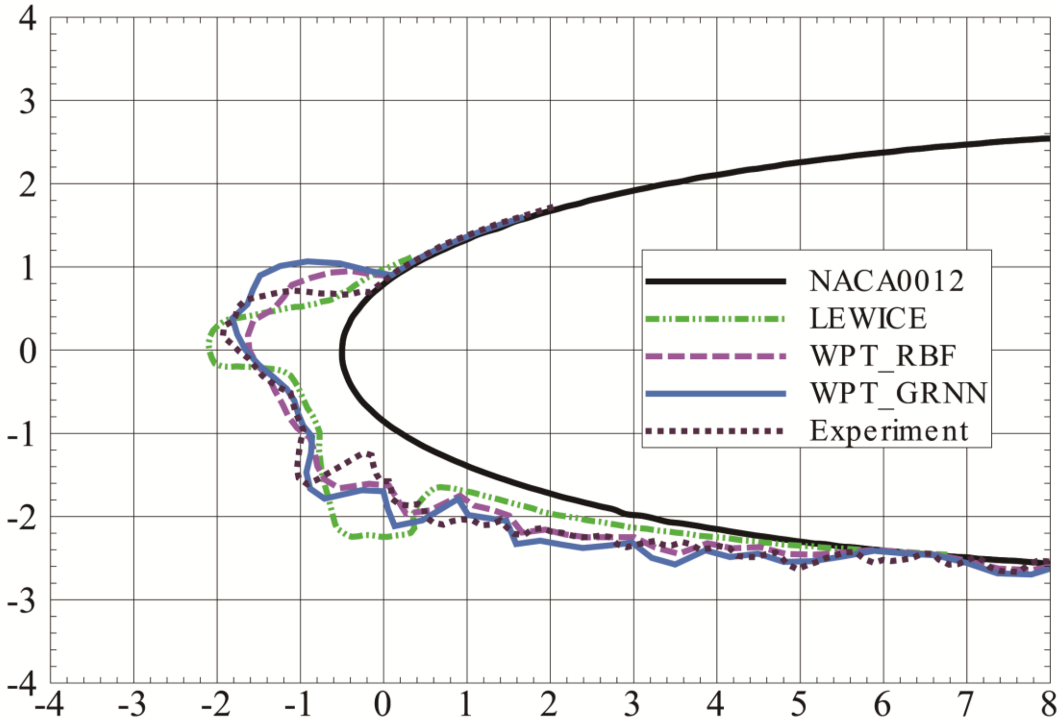

Fig. 13. Comparison of the glaze ice1 shapes of the experimental, LEWICE and present RBF and GRNN result.

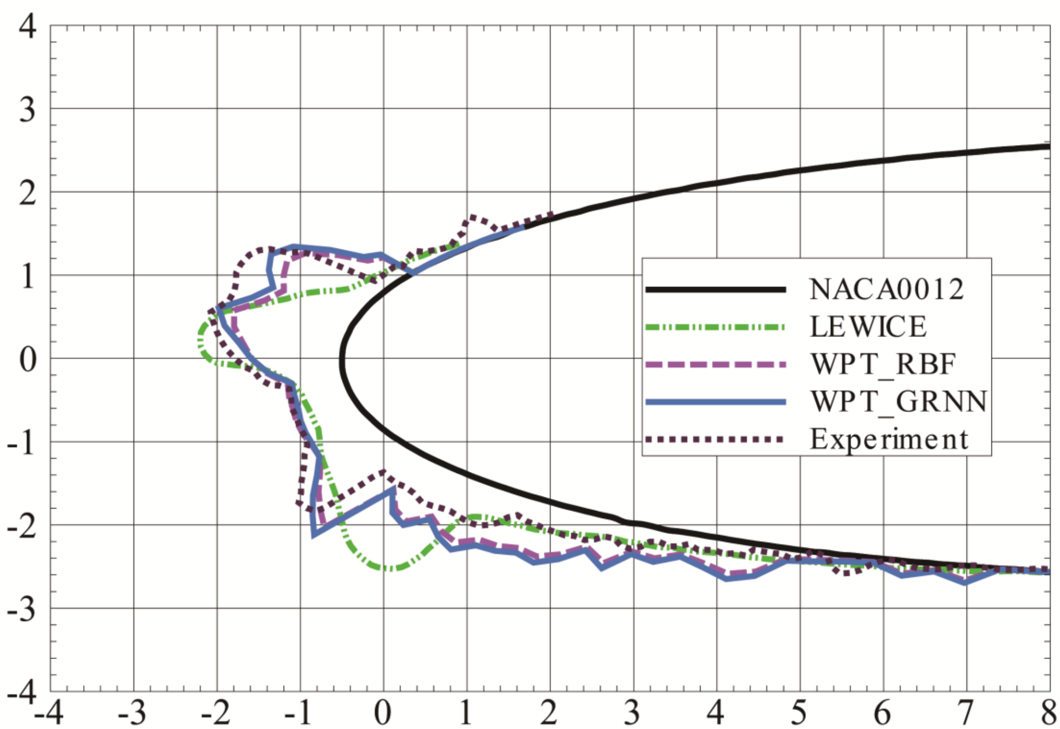

Fig. 14. Comparison of the glaze ice2 shapes of the experimental, LEWICE and present RBF and GRNN result.

For rime ice cases, as shown in Figs. 11 and 12, the overall shape and the extent of the ice accretion are both well predicted except for the ice mass which is slightly small. A close look at the glaze ice shape in Figs. 13 and 14, the angles of the upper and lower ice horns are fairly well captured. The distribution of the ice thickness over the surface is also reasonably predicted and the roughness of the experimental ice is well agreed. From the quantitative comparison shown in Table 3, it can be seen that the RBF should be considered as a first attempt at applying this technique to ice shape prediction when using the whole set of specimens.

Table 3

Summary of area-weighted errors when using the whole specimens.

Ice type	Data file number	LEWICE Area error(%)	RBF Area error(%)	GRNN Area error(%)
Rime ice1	JULY 1996 20736	35.40	24.83	18.51
Rime ice2	JULY 1991 27-6-36	27.70	21.74	24.31
Glaze ice1	JULY 1996 21236	28.43	21.56	24.57
Glaze ice2	JULY 1996 21336	28.23	27.34	29.76

4. Conclusions

In the present study, a combined wavelet packet transform (WPT) and artificial neural network (ANN) method is proposed for predicting the ice accretion on the surface of NACA0012 airfoil. Three different neural networks are proposed to predict the ice shape, and they are the commonly used back-propagation network (BP), radial basis function network (RBF), and generalized regression neural network (GRNN). Compared with the other two networks (BP and RBF), the GRNN can achieve overall better performance when the separated-specimen method is considered. Whereas the RBF network achieves better performance for the case of using the whole set of specimens. Results also show that the WPT-based method is in better qualitative agreement with the experiments than the LEWICE and Fourier-expansion-based method regarding the ice horns and the surface details of the glaze ice. It needs to be stressed that the database does not need to be separated in advance, since the neural network shows the same or even better performance when given the whole set of specimens for prediction. The proposed approach/software can be easily performed once the experimental data are available. Future work will extend the input parameter set to account for different variables, such as the chord length and angle of attack.

Acknowledgments

The authors would like to thank National Natural Science Foundation of China for the financial support in this research project (Grants No. 10872020 and 11072019).

References

[1] Lynch FT, Khodadoust A. Effects of ice accretions on aircraft aerodynamics. Progr Aerosp Sci. 2001;37:669-767.

[2] Ratvasky TP, Barnhart BP, Lee S. Current methods modeling and simulating icing effects on aircraft performance, stability, control. J. aircraft. 2010;47:201-11.

[3] Messinger BL. Equilibrium Temperature of an Unheated Icing Surface as a Function of Air Speed. J. Aeronautical Sciences (Institute of the Aeronautical Sciences). 1953;20:29-42.

[4] Myers TG. Extension to the Messinger model for aircraft icing. AIAA journal. 2001;39:211-8.

[5] Bragg MB, Broeren AP, Blumenthal LA. Iced-airfoil aerodynamics. Progr Aerosp Sci. 2005;41:323-62.

[6] Kind R, Potapczuk M, Feo A, Golia C, Shah A. Experimental and computational simulation of in-flight icing phenomena. Progr Aerosp Sci. 1998;34:257-345.

[7] Mingione G, Brandi V. Ice accretion prediction on multielement airfoils. J. Aircraft. 1998;35:240-6.

[8] Habashi WG. Recent Advances in CFD for In-Flight Icing Simulations. Japan Society of Fluid Mechanics. 2009;28:99-118.

[9] Nakakita K, Nadarajah S, Habashi W. Toward Real-Time Aero-Icing Simulation of Complete Aircraft via FENSAP-ICE. J. Aircraft. 2010;47:96-109.

[10] Fossati M, Habashi WG. Multiparameter Analysis of Aero-Icing Problems Using Proper Orthogonal Decomposition and Multidimensional Interpolation. AIAA journal. 2013;51:946-60.

[11] Jung SK, Shin S, Myong RS, Cho TH. An efficient CFD-based method for aircraft icing simulation using a reduced order model. J. Mechani. Sci. Techno. 2011;25:703-11.

[12] Ogretim E, Huebsch WW, Shinn A. Aircraft ice accretion prediction based on neural networks. J. Aircraft. 2006;43:233-40.

[13] Melody JW, Pokhariyal D, Merret J, Basar T, Perkins W, Bragg M. Sensor integration for inflight icing characterization using neural networks. AIAA paper, 2001-0542.; 2001.

[14] Fan HY, Lu WZ, GUANG X, Wang SJ. An improved neural-network-based calibration method for aerodynamic pressure probes. J. Fluids Eng. 2003;125:113-20.

[15] McCann DW. NNICE–a neural network aircraft icing algorithm. Environmental Modelling & Software. 2005;20:1335-42.

[16] Cao Y, Yuan K, Li G. Effects of ice geometry on airfoil performance using neural networks prediction. Aircraft Eng. Aerosp. Technol.. 2011;83:266-74.

[17] Mallat S. A Wavelet Tour of Signal Processing: The Sparse Way Burlington: Academic Press; 2008.

[18] Han JG, Ren WX, Sun ZS. Wavelet packet based damage identification of beam structures. Int. J. Solids Structures. 2005;42:6610-27.

[19] Liu Y-Y, Ju Y-F, Duan C-D, Zhao X-F. Structure damage diagnosis using neural network and feature fusion. Eng. Appli. Artificial Intelligence. 2011;24:87-92.

[20] Daqrouq K. Wavelet entropy and neural network for text-independent speaker identification. Eng. Appli. Artificial Intelligence. 2011;24:796-802.

[21] Vong C-m, Wong P-k, Ip W-f. Case-based expert system using wavelet packet transform and kernel-based feature manipulation for engine ignition system diagnosis. Eng. Appli. Artificial Intelligence. 2011;24:1281-94.

[22] Ogretim E, Huebsch WW. A novel method for automated grid generation of ice shapes for local‐flow analysis. Int. J. Numer. Methods Fluids. 2004;44:579-97.

[23] Wright WB. A summary of validation results for LEWICE 2.0: National Aeronautics and Space Administration, Lewis Research Center; 1998.